ARTICLES
PUBLISHED ONLINE: 8 DECEMBER 2013 | DOI: 10.1038/NPHOTON.2013.315
nature photonics

Laser streaking of free electrons at 25 keV

F. O. Kirchner[1,2], A. Gliserin[1,2], F. Krausz[1,2] and P. Baum[1,2]*

Recording electronic motion in atomic systems requires attosecond and picometre resolutions. Current attosecond technology provides photon pulses up to an energy range of 100 eV, with wavelengths far too long to access structures on the atomic scale. In contrast, ultrashort free-electron pulses with sub-Ångstrom de Broglie wavelengths offer the potential to resolve sub-atomic structures. Here, we demonstrate an optical-field-driven streak camera for their temporal characterization. Our concept is to have an electron beam and a laser beam intersect at an ultrathin metal mirror, and potentially offers attosecond resolution. The technique will be instrumental in advancing ultrafast electron diffraction towards ever higher temporal resolution in the pursuit of the long-term goal of sub-atomic four-dimensional imaging. As a first application, we study the influence of electron–electron interactions on the characteristics of few-electron pulses.

Capturing electrons in motion is at the heart of attosecond science. Although attosecond spectroscopy[1–4] can provide insight into the dynamical evolution of some observables of electrons in atomic systems, direct access to their spatial distribution is difficult. High-harmonic orbital tomography[4–7] and laser-induced self-diffraction[8,9] have been the first techniques to combine atomic resolution in space with time resolution on the electronic scale. However, both approaches suffer from the presence of a strong field and have been restricted to the scrutiny of simple systems only.

Ultrafast electron diffraction with freely propagating electron pulses at tens of keV and beyond[10–13] offers a powerful route to time-resolving dynamics with sub-atomic-scale spatial resolution. The de Broglie wavelength is 1–10 pm and tens of Bragg spots are observable at the same time, providing picometre resolution of complex organic molecules or unit cells. The temporal resolution is of the order of several hundred femtoseconds, measured by ponderomotive scattering[14,15] and limited by space-charge effects in multi-electron packets[11,16]. This limitation may possibly be overcome by utilizing the linear chirp of multi-electron[17] or single-electron[18–20] pulses, offering the potential for shortening the electron pulse duration by microwave compression, as proposed in ref. 21 and implemented in ref. 16, ultimately into the subfemtosecond regime[22].

Reliable electron pulse metrology with sufficient time resolution is a key prerequisite for exploiting this potential. Here, we demonstrate a temporal characterization technique with potentially subfemtosecond resolution. Our concept draws on that of the attosecond streak camera: abrupt release of bound electrons via extreme-ultraviolet-induced photoemission[1] into a laser field allows the moment of electron birth in the field to be labelled with a change in their final momentum[23]. Implementation of the concept with controlled laser fields[24] permits precision measurement of attosecond extreme-ultraviolet pulses and the laser fields themselves[25]. We demonstrate the extension of this measurement concept to electrons entering the optical streaking field as freely propagating beams. We refer to them as free electrons to emphasize the difference with respect to the photoelectrons ejected into the laser field from bound states in previous implementations of laser streaking. The ability to characterize high-energy freely propagating electron pulses with potentially subfemtosecond resolution opens the door to advancing time-resolved single-electron diffraction towards the 1 fs frontier, and possibly beyond.

Light-field-induced energy change of free electrons

A free electron of substantial energy can efficiently exchange energy with a laser field if it abruptly enters (or exits) a region of space where the laser field already oscillates with non-zero amplitude, that is, without having to traverse regions with slowly increasing (or decreasing, respectively) field amplitude (condition (1)). The resultant maximum energy exchange is proportional to the initial electron momentum and the component of the field amplitude along this momentum at the instant of electron launch (or exit); ponderomotive corrections quadratic in the field[26] are usually negligible. The energy exchange is also critically dependent on the timing of the electron with respect to field oscillations, offering a means of temporal characterization with potentially subfemtosecond resolution. For this potential to be exploited, two more conditions must be met: (2) the velocity of the electron's point of appearance/disappearance in the laser wave must match the field's phase velocity in the relevant interaction volume and (3) the interaction must be reproducible for statistical averaging at each laser-electron delay. In order that this averaging preserves the attosecond temporal resolution potentially offered by the temporal gradients of visible-to-infrared light, it must be ensured that a subfemtosecond electron wave packet is launched into the field at precisely the same phase of the field in repeated interactions.

In attosecond streaking of electrons released from bound atomic states[25], all three conditions (1) to (3) are met in a natural way by collinear propagation (both at the vacuum speed of light) of the sub-laser-cycle-duration extreme-ultraviolet pulse releasing the photoelectrons with a phase-controlled streaking laser field previously used for the generation of the extreme-ultraviolet pulse[24] and thereby avoiding any notable timing jitter in repeated measurements. Extension of this attosecond temporal characterization technique from electrons ejected from atomic bound states to ones freely propagating across the streaking laser beam is non-trivial, for two reasons. First, the electrons gradually propagate into the interaction region rather than being 'born' in it and, second, they do so with a velocity substantially slower than the phase velocity of the light wave.

We satisfy condition (1) by having a femtosecond laser beam reflected off a thin metal film and have it intersected with the electron beam traversing the film (Fig. 1a). A similar geometry was previously used for electron acceleration[27]. Thanks to the nanometre scale, that is, subwavelength penetration depth of the field into the metal foil,

[1]Max-Planck-Institute of Quantum Optics, Hans-Kopfermann-Strasse 1, 85748 Garching, Germany, [2]Ludwig-Maximilians-Universität München, Am Coulombwall 1, 85748 Garching, Germany. *e-mail: peter.baum@lmu.de

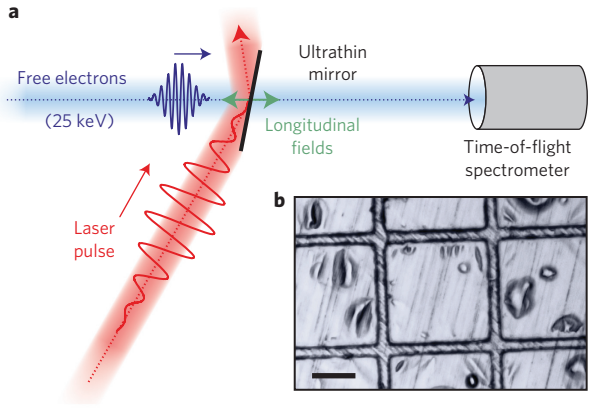

Figure 1 | Concept for attosecond streaking of freely propagating electron pulses at 25 keV. a, A laser pulse (red) and an electron pulse (blue) intersect at an ultrathin metal mirror (black) that is transparent to the electrons. The noncollinear geometry provides laser fields in forward and backward directions along the electron trajectory (green). The transition of the electrons out of the field occurs within 200 as, which is less than half an optical cycle. This makes a streak camera with a resolution given by the field oscillations. **b**, Microscopic image of the freestanding aluminium film with a thickness of 50 nm. Scale bar, 100 μm.

the electrons abruptly leave the field, just as the photoelectrons enter it in a 'conventional' attosecond streak camera.

Ultrashort electron pulses suitable for diffraction at ultimate resolutions come as collimated beams with diameters of hundreds of micrometres. To produce longitudinal field components along the electron momentum direction, we use a non-collinear interaction geometry (Fig. 1a). At a correct choice of angles, this geometry also fulfills requirement (2); that is, the electron hits the film at a well-defined delay with respect to the oscillating laser field, irrespective of its transverse position within the electron beam. Condition (3) can be readily fulfilled by implementing the concept with phase-controlled laser pulses[24].

Reflection of the p-polarized laser pulse at a mirror creates a transient standing wave with its electric and magnetic fields pointing normal and parallel to the surface, respectively. The electric field component parallel to the electron momentum (Fig. 1a, green arrows) is primarily responsible for energy exchange. Equipped with a metal film of carefully optimized properties and supplemented with a high-resolution energy analyser, this scheme constitutes an attosecond streak camera for free electrons.

Laser-field-driven streaking of free-electron pulses

The electron pulses to be characterized by the above system are generated from a femtosecond-laser-driven electron gun and accelerated in a static electric field to 25 keV. The absolute and relative bandwidths of the released electron pulses are ~0.4 eV and $\sim 1 \times 10^{-5}$, respectively. The streaking laser pulses are carried at a wavelength of $\lambda = 800$ nm, have a duration of ~50 fs, a peak intensity of ~0.4 TW cm^{-2} and exhibit a random carrier-envelope phase. The free-standing aluminium foil of the streak camera has a thickness of 50 nm and is supported on a gold mesh (Fig. 1b). Energy analysis is performed with a home-built time-of-flight spectrometer providing a resolution of ~1 eV at 25 keV.

In the single-electron regime, the electron pulse duration (relevant, for example, to laser-pump/electron-probe experiments) is defined as the statistical deviation of the arrival time of the electrons with respect to their nominal arrival time. This random deviation arises from a random initial electron energy implying a spread in arrival time at the target. In the language of quantum mechanics, this spread can be described by a wave packet of corresponding longitudinal extension. In our experiment, the electron pulse duration is anticipated to be several hundred femtoseconds[20]. The laser–electron interaction is then expected to yield sidebands in the electron energy spectrum rather than a definite shift in energy, similarly to photon-assisted electron microscopy[28–31], to field-driven emission from needle sources[32] and to attosecond streaking of electron wave packets longer than the streaking field cycle[2].

For a first proof-of-principle experiment of free-electron streaking we generated about three electrons per pulse to achieve good detection statistics. Figure 2 shows the measured spectrogram in the time-energy domain, that is, a series of electron spectra as a function of the laser-electron delay. For negative delays the electron pulses arrive at the aluminium foil before the laser pulses. In the proximity of zero delay, where laser and electron pulses overlap in time, electrons are redistributed from their original energy to higher and lower energies. The spectrogram reveals three conspicuous features: a time-dependent energy exchange, a temporal structure varying with the amount of energy gain/loss, and pronounced interferences in the energy domain, subject to shifts versus delay.

Amount of energy gain/loss

For the experimental conditions presented in Fig. 2, the highest energy gain extends up to ~65 eV. In conventional streaking, the maximum energy gain transferred from the optical field to the electron can be calculated using a semiclassical approach[2] as

$$\Delta W_{\max} = \frac{e\lambda}{\sqrt{2m_e}\pi c}\sqrt{W_0}E_{\max} \qquad (1)$$

where W_0 is the electron's initial energy, e and m_e are the electron's charge and mass, respectively, and $E_{\max}$ is the peak of the laser's electric field along the trajectory of the electron.

To apply equation (1) to our free-space geometry, we must consider the optical interference at the metal. In addition, magnetic fields are non-negligible at an electron velocity of ~0.3c. Standing-wave interference at the aluminium film produces an increase in the electric and magnetic fields at the surface by

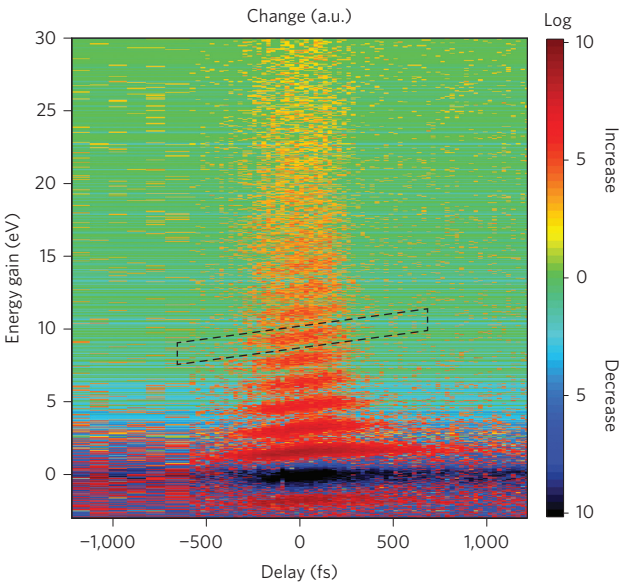

Figure 2 | Streaking results. Energy change of electron pulses at 25 keV depicted in dependence on the delay of the optical streaking pulses. The spectrogram reveals a time-dependent energy transfer, interference features with a tilt, and an energy-dependent temporal width. The spectrum of the unstreaked electrons is subtracted. Dashed box, region of interest for data analysis.

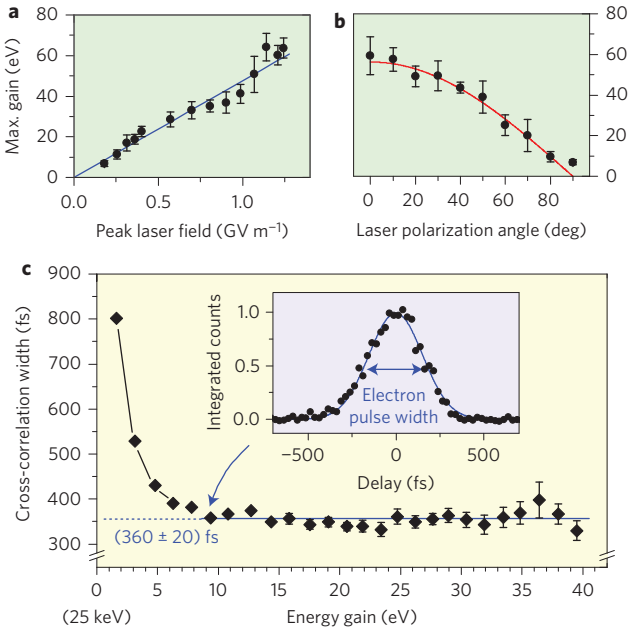

Figure 3 | Field dependence and electron pulse characterization. a, Streaking is field-dependent. Measurement of the highest energy change in dependence on the applied laser field (symbols) shows a linear behaviour (blue line). **b**, Streaking requires longitudinal fields. Measurement of the highest energy change in dependence on the polarization (symbols) shows a cosine-type behaviour (red line) peaking at p-polarization. **c**, Temporal widths of the spectrogram and electron pulse shape. Measurement of the cross-correlation widths (diamonds, FWHM) for increasing energy gain shows a rapid decrease towards a limit of 360 fs. This denotes the electron pulse duration. Inset: electron pulse shape (symbols), sampled at an energy gain of 9 eV. The electron pulse is approximately Gaussian-shaped (blue).

~50%. From the perspective of the electron beam, the electric field has a longitudinal component (responsible for energy change) and a transverse component (deflecting the beam sideways). For the chosen combination of angles, the latter is compensated almost completely by the magnetic part of the Lorentz force. With the experimental laser parameters and the optical properties of the aluminium film, we calculate a maximum energy gain of 73 eV. This is in good agreement with the experimental findings, showing that equation (1) is still valid at 25 keV, provided that optical interferences and magnetic components are properly taken into account. An easily measurable energy gain of several electronvolts can be generated at the substantially weaker fields achievable with nanojoule pulse energies. Hence, the technique presented here can be implemented with pulses directly from femtosecond laser oscillators, without the need for amplification.

Interaction driven by the oscillating fields

In contrast with ponderomotive effects[26], laser streaking is expected to induce changes in the final observables that scale with the field amplitude rather than the cycle-averaged intensity. Figure 3a shows the maximum energy gain of the streaked electrons versus peak laser field strength. The change in maximum energy gain is linearly proportional to the peak electric field, as predicted by equation (1). Figure 3b shows the dependence of the electrons' maximum energy gain on laser polarization. Zero degrees indicates polarization in the plane of incidence, where the electric field components into and out of the film are maximized. The solid line is a least-square fit using a cosine function. The measurement clearly reveals the dominant role of the longitudinal component for the streaking effect. These experiments provide a clear testimony for the laser–electron interaction being controlled by the instantaneous fields rather than the (cycle-averaged) ponderomotive potential.

Interference effects

The spectrogram in Fig. 2 shows a pronounced interference in the energy domain. Within the spectral window in which the time-of-flight detector is optimized for highest resolution, about ten maxima are perceivable in the gain region and one in the loss region. Distinct features are no longer discernible at higher energy gains owing to the limited energy resolution of the detection system in this range. The measured separation is equidistant at ~1.6 eV, which is close to the laser's photon energy of $E_{photon} \approx$ 1.55 eV at $\lambda \approx 800$ nm. We call these features streaking traces of different order, or 'streaking orders'.

Similar sidebands in the energy spectrum of free electrons have been observed with electron microscopy in the vicinity of nanostructures[28,29,31]. These were explained in terms of multiphoton absorption moderated by the near-field around the nanostructure[29,31]. Here, we offer an explanation from a different, semiclassical perspective in terms of electron–wave interferences induced by a classical light field[33]. The energy bandwidth (full-width at half-maximum, FWHM) of our unstreaked electron pulses was measured as ~0.4 eV, implying a (propagation-induced) broadening of the single-electron wave packets to a duration much longer than the period of the streaking optical field. Electrons leaving the field in subsequent cycles and gaining or losing the same energy can therefore interfere, giving rise to sidebands separated by the photon energy, similar to those appearing in above-threshold ionization[34]. The visibility of the spectral fringes related to the streaking orders is dictated by the temporal coherence of the electron pulse.

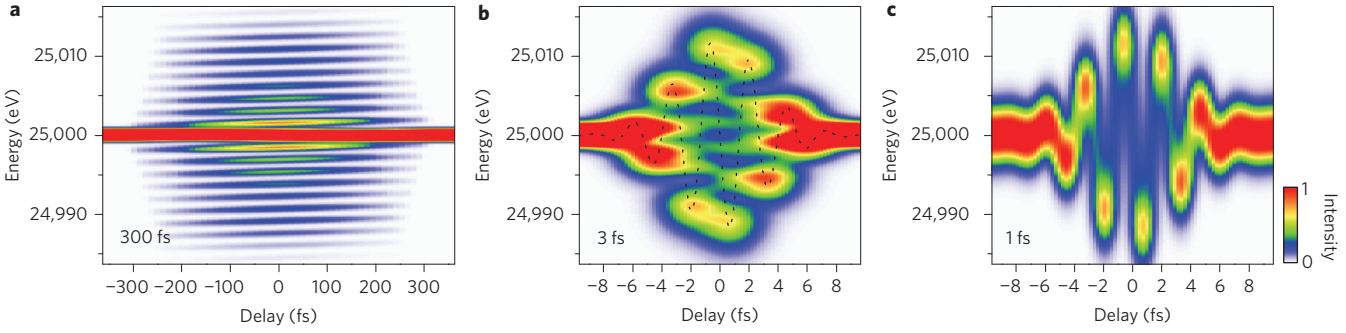

Figure 4 | Semi-classical simulations of free-electron streaking. a, A case for chirped electron pulses (300 fs, FWHM) reproduces the tilted interference orders and the field dependence of the experiments. **b**, Application of phase-stabilized 5 fs laser pulses (dotted line) and 3 fs electron pulses shows the transition regime between coherent interference and field-resolved sampling. **c**, Assuming 1 fs electron pulses, the spectrogram turns into a direct sampling of the 5 fs laser field.

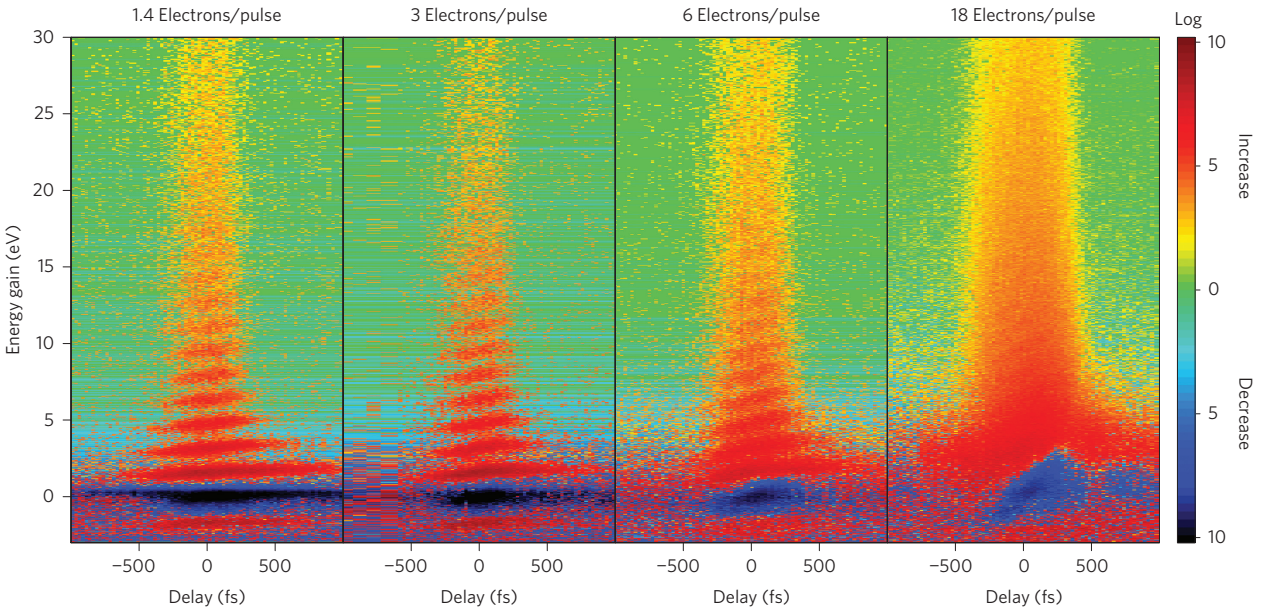

Figure 5 | Multi-electron dynamics in freely propagating electron pulses. Streaking spectrograms for an average of 1.4, 3, 6 and 18 electrons per pulse reveal an increase of pulse duration, chirp and bandwidth, as well as a loss of interference contrast.

Currently, it is limited by the energy resolution of the detection system. From the observed fringe visibility we can therefore only evaluate a lower limit for the electron's temporal coherence: it must extend over at least two laser cycles, corresponding to a minimum of 1×10^4 coherent de Broglie cycles.

Streaking orders

For each streaking order, the temporal profile is a cross-correlation between the electron pulse and those parts of the laser pulse where the electric field exceeds the threshold for the respective energy gain according to the scaling given by equation (1). Thus, for higher streaking orders, the electron pulse is sampled with an effective probe of decreasing duration. In the limit of the highest streaking orders, near the maximum energy gain, the signal's delay dependence is expected to mirror the electron pulse shape. Figure 3c depicts the measured temporal widths of the spectrogram for increasing energy gains. The duration of the streaking traces of increasing order decreases rapidly and converges to an FWHM value of (360 ± 20) fs, yielding the electron pulse duration.

For low energy gains, the streaking orders become substantially wider and also asymmetric in time. The broadening is caused by the complex temporal profile of our laser pulses, which have a non-Gaussian spectrum and hence carry some pedestal in the range of ± 300 fs. The integrated intensity is less than 1%, but the corresponding field strength is still sufficient to cause some low-order streaking. The asymmetry is attributed to the uncorrected third-order dispersion in our laser system[35], which produces an asymmetric temporal profile of the pedestal.

The peak energy of the streaking traces exhibits a shift versus delay, both in the gain and loss region (Fig. 2). The shift is indicative of a temporal variation of the electron energy, that is, the electron pulse's chirp. We evaluate a chirp of (1.6 ± 0.2) eV ps^{-1}; the sign is such that higher-energy electrons arrive earlier at the streaking location than slower ones.

Semiclassical modelling

To verify the key features of our streaking experiment theoretically and to reveal its applicability to subfemtosecond electron pulses, we performed simulations using a time-dependent semiclassical approach with chirped single-electron pulses. Figure 4 shows the results for three cases, one resembling the measurement (50 fs laser pulses, 300 fs electron pulses, chirp of 1.6 eV ps^{-1}; all durations defined as FWHM values) and two cases assuming a phase-locked 5 fs laser pulse and electron pulses with durations of 3 fs and 1 fs, respectively. The pattern in Fig. 4a reproduces the expected proportionality of the streaking strength, the quantum interference, the tilt of the features resulting from electron chirp, and the convergence of the time width to the electron pulse duration for highest streaking energies.

Figure 4b,c shows what can be expected with a 5 fs laser pulse and electron pulses approaching the attosecond regime. There is a gradual transition between such spectrograms dominated by quantum interference, where the electrons extend over several laser cycles coherently (Fig. 4a), towards a streaking spectrogram indicative of electron pulses of sub-laser-cycle duration (Fig. 4c). Attosecond metrology offers a range of deconvolution methods with which the laser field and the electron's wavefunction can be retrieved[36,37]. Even without computational reconstruction, streaking spectroscopy provides direct insight into the temporal behaviour of ultrashort electron pulses in terms of pulse shape, duration, bandwidth, chirp and coherence.

First application: multi-electron dynamics in free space

As a first application, we make use of the streaking effect to reveal the influence of multi-electron dynamics on the chirp, bandwidth and duration of few-electron pulses in free space. We concentrate on the transitional regime between single electrons and the space-charge domain of continuous electron density. Figure 5 shows the data obtained for average values of 1.4, 3, 6 and 18 electrons per pulse. After the streaking mirror there is less than one electron in all cases; the measurement therefore characterizes the few-electron pulses at the location of the foil. The spectrograms differ in several notable aspects—electron pulse duration, bandwidth and chirp increase with number of electrons (Table 1), while the visibility of the streaking features decreases.

Coulomb repulsion enlarges the propagation-induced chirp of single-electron pulses[20] and produces an additional broadening in duration and bandwidth. The results for 1.4 and 3 electrons do not differ significantly, but only 18 electrons are enough to cause a sevenfold increase in bandwidth and a 50% increase in pulse

Table 1 | Results of streaking measurements on multi-electron pulses. Even for very few electrons per pulse, duration and bandwidth degrade notably.

Average no. of electrons	Pulse duration (fs, FWHM)	Energy bandwidth (eV, FWHM)	Electron chirp (eV ps^{-1})
1.4	360±20	0.39±0.06	1.1±0.2
3	370±30	0.58±0.03	1.6±0.2
6	390±20	1.01±0.08	2.6±0.2
18	540±20	2.9±0.2	5.4±0.4

duration. These results reflect the conversion of the initial electrostatic self-energy to a velocity spread with order-of-magnitude agreement with model predictions. At all electron densities, the chirp is found to be approximately linear, as predicted in the regime of a continuous space-charge density[17]. Hence, this approximation seems applicable, even for a very low number of electrons. The streaking interferences show an intriguing degradation of contrast. This may be a result of limitations in the experimental resolution of strongly tilted streaking orders, or indicative of a quantum-statistical loss of temporal coherence by electron–electron interactions during propagation before the characterization at the foil. Shorter laser pulses and an improvement of energy resolution will allow this question to be resolved. For practical applications, a noteworthy result is that tens of electrons per pulse already markedly affect the temporal resolution of a femtosecond diffraction experiment. Because Coulomb repulsion becomes more severe with shorter pulses after compression[22], this underlines the significance of the genuine single-electron regime for achieving ultimate resolutions.

Outlook

We have extended the technique of laser streaking to freely propagating electron pulses at an energy of 25 keV, more than a hundred times higher than previously demonstrated in attosecond spectroscopy. Extension of our concept to the characterization of MeV pulses[38–41] is straightforward, provided that an energy spectrum can be measured with sufficient resolution. Simulations indicate the applicability of the laser-field streaking technique to attosecond electron pulses, laying the groundwork for gradually shortening the duration of single-electron pulses into the subfemtosecond regime for subatomic visualization of electronic motion in four dimensions.

Materials and methods

Beams. A long-cavity Ti-sapphire oscillator[35] was operated at 128 kHz using a pulse picker. A small portion of the laser power was frequency-tripled and focused tightly onto a gold-coated photocathode[42]. Femtosecond electron pulses were created and accelerated to 25 keV over a distance of 3 mm. A solenoid lens produced a roughly collimated beam with dimensions of 323 × 288 μm^2 (FWHM). The number of electrons per pulse was estimated from the count rate, foil transmission, detector efficiency and repetition rate. The major part of the laser power was focused onto the streaking mirror (beam waist, 44 × 68 μm^2, FWHM) under a shallow angle. The pulse duration was ~50 fs (FWHM). The p-polarized laser beam and the electron beam impinged at angles of incidence of 77° and 17°, respectively, to match the electron's group velocity (about 0.3c) to the optical phase velocity along the surface. The electron pulse hit the film at each point within the beam profile at the same delay relative to the laser field.

Streaking element. The foil had to be thick enough to block the laser pulses, but thin enough to transmit the electrons. Aluminium simultaneously provides good optical reflectivity and low atomic mass, facilitating electron transmission. A 50 nm layer of aluminium was thermally evaporated onto a soap-covered glass substrate. The soap was removed with water and the film transferred to a 100-lines-per-inch mesh for support. The foil transmitted ~3.5% of the incident electron current.

Time-of-flight detector. A drift-tube (40 mm inner diameter, 200 mm length) was operated at ~24,995 V and the timing was detected with a microchannel plate. For calibration, the acceleration voltage was varied while recording the time-of-flight spectrum of the direct electron beam. Streaking spectrograms in energy units were obtained using the calibrated time-to-energy mapping, $t(E)$. Finally, the intensity was weighted by $\mathrm{d}t(E)/\mathrm{d}E$ to account for the nonlinear relation between the respective bin sizes. The achieved energy resolution was better than 0.5 eV (FWHM) within ±3 eV around the central energy and better than 1 eV (FWHM) up to 13 eV above the central energy.

Analysis. Individual streaking orders were selected using skewed regions of interest (ROI, Fig. 2); equally shaped ROI were applied at higher energies. We fit the data along the energy axis with Gaussian functions, providing the centre and amplitude for each delay time. A Gaussian fit of the amplitude values yielded the duration of the electron-laser cross-correlation. The slope of the streaking orders was obtained by fitting a linear function to the fitted centre positions. The energy bandwidth was retrieved by multiplying cross-correlation durations and corresponding slope values. The temporal profile (Fig. 3c, inset) was obtained by integrating a ROI along the energy axis. The error bars in Fig. 3c represent the standard errors of Gaussian fits to these profiles. The electron pulse duration and its uncertainty were obtained as mean value and standard deviation of temporal profile widths in the convergence region. Chirp values were obtained by dividing energy bandwidth by pulse duration. The error bars in Fig. 3a,b reflect the uncertainty of the transition between counts and noise defining the cutoff energy.

Simulations. The electron was treated as a non-relativistic quantum wave packet in a classical laser field using atomic units[33]. Spatial effects were neglected in our one-dimensional approach. A single electron wavefunction is given by $\exp[-t^2/(2\xi^2)]\exp(-iUt)$, where U is the central energy and ξ is the coherence time. The time-dependent density of electrons is $I_{\mathrm{el}}(t) \propto \exp(-t^2/(2\tau_{\mathrm{el}}{}^2))$, where τ_{el} is the pulse duration (sigma value). Chirp is described by a time-dependent energy $U(t_{\mathrm{el}}) = U_0 + Ct_{\mathrm{el}}$. For simulating spectrograms, it is sufficient to know the laser field's time-dependent effective potential $A(t)$ at the location of the foil; this comprises the net effect of electromagnetic acceleration and deceleration during spatiotemporal propagation that far. We use $A(t) = A_0\exp[-t^2/(2\tau_{\mathrm{field}}{}^2)]\exp(i\omega t)$, where τ_{field} is the duration of the field (sigma value), $\omega = 0.057$ is the central frequency and $A_0 = 0.012$ is the peak potential. Each single-electron wave packet in the long electron pulse interacts with the laser individually and we assume that collision with the foil is instantaneous. With these approximations, the energy spectrum $S(U)$ of one electron within the pulse is[33]

$$S(U, t_{\mathrm{el}}) \propto \frac{1}{\sqrt{U}}\left|\int_{-\infty}^{\infty}\exp\left(-\frac{(t-t_{\mathrm{el}})^2}{2\xi^2} - i(U_0 + Ct_{\mathrm{el}})t + i\phi(U, t_{\mathrm{el}})\right)\mathrm{d}t\right|^2 \quad (2)$$

where ϕ is the classical action in the laser potential given by the Volkov-type phase $\phi(U, t_{\mathrm{el}}) = \frac{1}{2}\int_{-\infty}^{t_{\mathrm{el}}}[\sqrt{2U} + A(t)]^2\mathrm{d}t$. We can neglect contributions scaling with A^2, because the expected energy change is small compared to U_0. Hence, equation (2) can be simplified to

$$S(U, t_{\mathrm{el}}) \propto \frac{1}{\sqrt{U}}\left|\int_{-\infty}^{\infty}\exp\left(-\frac{(t-t_{\mathrm{el}})^2}{2\xi^2} - i(U_0 + Ct_{\mathrm{el}})t + i\sqrt{2U}\int_{-\infty}^{t_{\mathrm{el}}}A(t')\mathrm{d}t'\right)\mathrm{d}t\right|^2. \quad (3)$$

Here the integral of the laser potential needs to be computed only once. The measured spectrum is a superposition of many such single-electron spectra in the pulse with density $I_{\mathrm{el}}(t)$. For a delay Δt between laser and electron pulses, we obtain

$$\tilde{S}(U, \Delta t) \propto \int_{-\infty}^{\infty} I_{\mathrm{el}}(t - \Delta t)S(U, t)\mathrm{d}t \quad (4)$$

This produces the streaking spectra shown in Fig. 4.

Received 1 August 2013; accepted 22 October 2013; published online 8 December 2013

References

1. Hentschel, M. *et al.* Attosecond metrology. *Nature* **414,** 509–513 (2001).
2. Drescher, M. *et al.* Time-resolved atomic inner-shell spectroscopy. *Nature* **419,** 803–807 (2002).
3. Niikura, H. *et al.* Probing molecular dynamics with attosecond resolution using correlated wave packet pairs. *Nature* **421,** 826–829 (2003).
4. Itatani, J. *et al.* Tomographic imaging of molecular orbitals. *Nature* **432,** 867–871 (2004).
5. Niikura, H. *et al.* Sub-laser-cycle electron pulses for probing molecular dynamics. *Nature* **417,** 917–922 (2002).
6. Baker, S. *et al.* Probing proton dynamics in molecules on an attosecond time scale. *Science* **312,** 424–427 (2006).
7. Smirnova, O. *et al.* High harmonic interferometry of multi-electron dynamics in molecules. *Nature* **460,** 972–977 (2009).

8. Meckel, M. *et al.* Laser-induced electron tunneling and diffraction. *Science* **320,** 1478–1482 (2008).
9. Blaga, C. I. *et al.* Imaging ultrafast molecular dynamics with laser-induced electron diffraction. *Nature* **483,** 194–197 (2012).
10. Flannigan, D. J. & Zewail, A. H. 4D electron microscopy: principles and applications. *Acc. Chem. Res.* **45,** 1828–1839 (2012).
11. Sciaini, G. & Miller, R. J. D. Femtosecond electron diffraction: heralding the era of atomically resolved dynamics. *Rep. Prog. Phys.* **74,** 096101 (2011).
12. Shorokhov, D. & Zewail, A. H. 4D electron imaging: principles and perspectives. *Phys. Chem. Chem. Phys.* **10,** 2879–2893 (2008).
13. Chergui, M. & Zewail, A. H. Electron and X-ray methods of ultrafast structural dynamics: advances and applications. *ChemPhysChem* **10,** 28–43 (2009).
14. Hebeisen, C. T. *et al.* Femtosecond electron pulse characterization using laser ponderomotive scattering. *Opt. Lett.* **31,** 3517–3519 (2006).
15. Hebeisen, C. T. *et al.* Grating enhanced ponderomotive scattering for visualization and full characterization of femtosecond electron pulses. *Opt. Express* **16,** 3334–3341 (2008).
16. Van Oudheusden, T. *et al.* Compression of subrelativistic space-charge-dominated electron bunches for single-shot femtosecond electron diffraction. *Phys. Rev. Lett.* **105,** 264801 (2010).
17. Siwick, B. J., Dwyer, J. R., Jordan, R. E. & Miller, R. J. D. Ultrafast electron optics: Propagation dynamics of femtosecond electron packets. *J. Appl. Phys.* **92,** 1643–1648 (2002).
18. Lobastov, V. A., Srinivasan, R. & Zewail, A. H. Four-dimensional ultrafast electron microscopy. *Proc. Natl Acad. Sci. USA* **102,** 7069–7073 (2005).
19. Zewail, A. H. Four-dimensional electron microscopy. *Science* **328,** 187–193 (2010).
20. Aidelsburger, M., Kirchner, F. O., Krausz, F. & Baum, P. Single-electron pulses for ultrafast diffraction. *Proc. Natl Acad. Sci. USA* **107,** 19714–19719 (2010).
21. Fill, E., Veisz, L., Apolonski, A. & Krausz, F. Sub-fs electron pulses for ultrafast electron diffraction. *New J. Phys.* **8,** 272 (2006).
22. Veisz, L. *et al.* Hybrid DC–AC electron gun for fs-electron pulse generation. *New J. Phys.* **9,** 451 (2007).
23. Itatani, J. *et al.* Attosecond streak camera. *Phys. Rev. Lett.* **88,** 173903 (2002).
24. Baltuska, A. *et al.* Attosecond control of electronic processes by intense light fields. *Nature* **421,** 611–615 (2003).
25. Kienberger, R. *et al.* Atomic transient recorder. *Nature* **427,** 817–821 (2004).
26. Bucksbaum, P. H., Bashkansky, M. & McIlrath, T. J. Scattering of electrons by intense coherent-light. *Phys. Rev. Lett.* **58,** 349–352 (1987).
27. Plettner, T. *et al.* Visible-laser acceleration of relativistic electrons in a semi-infinite vacuum. *Phys. Rev. Lett.* **95,** 134801 (2005).
28. Barwick, B., Flannigan, D. J. & Zewail, A. H. Photon-induced near-field electron microscopy. *Nature* **462,** 902–906 (2009).
29. Park, S. T., Lin, M. M. & Zewail, A. H. Photon-induced near-field electron microscopy (PINEM): theoretical and experimental. *New J. Phys.* **12,** 123028 (2010).
30. Yurtsever, A., van der Veen, R. M. & Zewail, A. H. Subparticle ultrafast spectrum imaging in 4D electron microscopy. *Science* **335,** 59–64 (2012).
31. Park, S. T., Kwon, O. H. & Zewail, A. H. Chirped imaging pulses in four-dimensional electron microscopy: femtosecond pulsed hole burning. *New J. Phys.* **14,** 053046 (2012).
32. Krüger, M., Schenk, M. & Hommelhoff, P. Attosecond control of electrons emitted from a nanoscale metal tip. *Nature* **475,** 78–81 (2011).
33. Reckenthaeler, P. *et al.* Proposed method for measuring the duration of electron pulses by attosecond streaking. *Phys. Rev. A* **77,** 042902 (2008).
34. Agostini, P., Fabre, F., Mainfray, G., Petite, G. & Rahman, N. K. Free-free transitions following 6-photon ionization of xenon atoms. *Phys. Rev. Lett.* **42,** 1127–1130 (1979).
35. Naumov, S. *et al.* Approaching the microjoule frontier with femtosecond laser oscillators. *New J. Phys.* **7,** 216 (2005).
36. Mairesse, Y. & Quere, F. Frequency-resolved optical gating for complete reconstruction of attosecond bursts. *Phy. Rev. A* **71,** 011401 (2005).
37. Quere, F., Mairesse, Y. & Itatani, J. Temporal characterization of attosecond XUV fields. *J. Mod. Opt.* **52,** 339–360 (2005).
38. Li, R. K. *et al.* Experimental demonstration of high quality MeV ultrafast electron diffraction. *Rev. Sci. Instrum.* **80,** 083303 (2009).
39. Tokita, S., Inoue, S., Masuno, S., Hashida, M. & Sakabe, S. Single-shot ultrafast electron diffraction with a laser-accelerated sub-MeV electron pulse. *Appl. Phys. Lett.* **95,** 111911 (2009).
40. Musumeci, P., Moody, J. T., Scoby, C. M., Gutierrez, M. S. & Westfall, M. Laser-induced melting of a single crystal gold sample by time-resolved ultrafast relativistic electron diffraction. *Appl. Phys. Lett.* **97,** 063502 (2010).
41. Muro'oka, Y. *et al.* Transmission-electron diffraction by MeV electron pulses. *Appl. Phys. Lett.* **98,** 251903 (2011).
42. Kirchner, F. O., Lahme, S., Krausz, F. & Baum, P. Coherence of femtosecond single electrons exceeds biomolecular dimensions. *New J. Phys.* **15,** 063021 (2013).

Acknowledgements

The authors thank D. Frischke for producing aluminium films, V. Yakovlev for discussions about coherence and streaking simulations, and S. Lahme for support with error analysis. The authors acknowledge funding from the European Research Council, the Munich Centre of Advanced Photonics, and the Rudolf-Kaiser Foundation. F.O.K. and A.G. are supported by the International Max-Planck Research School for Advanced Photon Science.

Author contributions

P.B. and F.K. conceived the streaking concept and F.O.K. investigated its feasibility. A.G. conceived and constructed the beamline and energy analyser. F.O.K. constructed the streaking interaction region. A.G. carried out a preliminary experiment and F.O.K. the final experiment. A.G. evaluated the analyser's output into spectrograms and F.O.K. analysed that data further. P.B. performed the semiclassical simulations. All authors interpreted the results. F.O.K. and P.B. created the figures. All authors wrote the paper. The total contributions of F.O.K. and A.G. were comparable.

Additional information

Reprints and permissions information is available online at www.nature.com/reprints. Correspondence and requests for materials should be addressed to P.B.

Competing financial interests

The authors declare no competing financial interests.